CHAPTER FIFTEEN

Scanning FCS for the Characterization of Protein Dynamics in Live Cells

Zdeněk Petrášek,[*,1] Jonas Ries,[*,1] *and* Petra Schwille[*]

Contents

Abstract

Scanning fluorescence correlation spectroscopy (sFCS) is the generic term for a group of fluorescence correlation techniques where the measurement volume is moved across the sample in a defined way. The introduction of scanning is motivated by its ability to alleviate or remove several distinct problems often encountered in standard FCS, and thus, to extend the range of applicability of fluorescence correlation methods in biological systems. These problems include poor statistical accuracy in measurements with slowly moving molecules, photobleaching, optical distortions affecting the calibration of the measurement

* Biotec, TU Dresden, Dresden, Germany
[1] Both authors contributed equally

Methods in Enzymology, Volume 472
ISSN 0076-6879, DOI: 10.1016/S0076-6879(10)72005-X

volume, membrane instabilities, etc. Here, we present an overview of sFCS methods, explaining their benefits, implementation details, requirements, and limitations, as well as relations to each other. Further, we give examples of different sFCS implementations as applied to cellular systems, namely large-circle sFCS to measure protein dynamics in embryo cortex and line sFCS to measure protein diffusion and interactions in unstable membranes.

1. Introduction

Fluorescence correlation spectroscopy (FCS) is a powerful tool to measure local concentrations, molecular weights, translational and rotational diffusion coefficients, chemical rate constants, association and dissociation constants, and photodynamics *in vitro* as well as *in vivo* (Bacia and Schwille, 2003; Bacia *et al.*, 2006; Kim *et al.*, 2007; Rigler and Elson, 2001). It is based on the statistical analysis of intensity fluctuations caused by fluorophores diffusing through a small (≈fL) detection volume (for details see Fig. 15.1) and requires only a low concentration (≈0.1–100 n*M*) of labeled molecules, minimizing the interference of the labeling with the system. The introduction of commercial confocal FCS systems has promoted the use of FCS so that it can now be considered a well-established technique. However, standard FCS suffers from several limitations of applicability, especially in complex biological systems. Optical artifacts (Enderlein *et al.*, 2005) such as

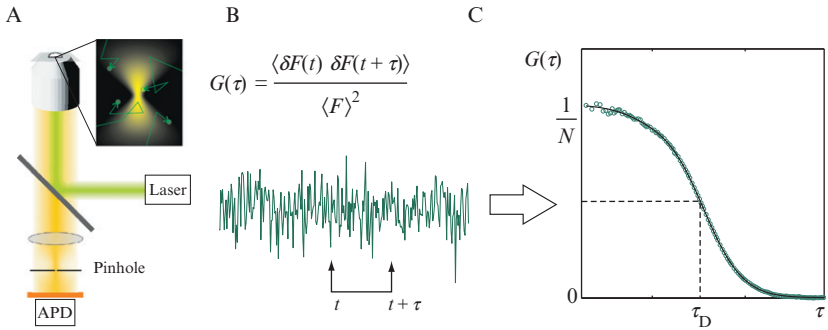

Figure 15.1 Principle of FCS. (A) The sample is illuminated by focusing the laser beam through an objective. The emitted photons are then spectrally filtered and detected with an avalanche photodiode. A pinhole provides axial confinement to result in a tiny (sub-femtoliter) detection volume. (B) Fluorophores diffusing through the detection volume give rise to a fluctuating intensity trace $F(t)$ from which the autocorrelation curve $G(\tau)$, which measures the self-similarity of the signal, can be calculated. (C) Parameters of interest, for example, the diffusion time τ_D or number of particles in the detection volume N, are obtained by fitting a mathematical model to the experimental correlation curve.

varying cover slide thickness, refractive index mismatch, optical saturation, or aberrations change the size of the detection volume, which precludes the precise calibration necessary for quantitative concentration or diffusion measurements. Slow diffusion in biological samples demands long measurement times—at least 10^5 times the slowest timescale found in the system (Tcherniak *et al.*, 2009)—and the long residence times in the detection volume promote photobleaching. Finally, measurements on biological membranes are especially challenging, since even tiny membrane movements or instabilities lead to severe artifacts.

To overcome these limitations, modifications of standard FCS have been developed (Dertinger *et al.*, 2007; Digman *et al.*, 2005; Ruan *et al.*, 2004), one of the most successful being sFCS (Petrášek and Schwille, 2008c). sFCS employs a moving detection volume instead of a static detection volume, which has several advantages (Box 1): sampling of a larger volume increases

Box 1 When to use sFCS

Decide whether to use standard FCS or sFCS. In the following situations sFCS may be superior to standard FCS:

- *Slow motion*. The molecules diffuse (or move) very slowly, with diffusion times in the range of tens (hundreds) of milliseconds or longer. There are not enough fluctuation events during the permissible measurement time and the calculated autocorrelation is too noisy, especially at long lag times. By scanning the sample, the measurement is performed at more locations, thus improving the statistics.
- *Optical distortions*. The measurement is performed within an optically inhomogeneous medium, such as cells or tissues, where the focused laser spot can be deformed, changing its size and shape. This invalidates the calibration of the volume size by an independent measurement, necessary in standard FCS to determine diffusion coefficients and particle numbers. Choose one of the types of sFCS where the volume calibration is replaced by an exact knowledge of the scan path. Small-circle sFCS is useful when the measurement has to be limited to a small part of the sample, while large-circle or line sFCS simultaneously improves the signal-to-noise ratio in case of slowly diffusing molecules by sampling a larger area.
- *Photobleaching*. Due to slow motion, the molecules stay too long in the laser focus and are more likely to become photobleached, resulting in distortions of the correlation curve. Choose a type of sFCS with a larger scan path, whereby more molecules are probed for a shorter time, thus reducing the risk of photobleaching and at the same time improving the statistics.

(continued)

Box 1 (continued)

- *Membrane motion*. When measuring motion on surfaces, for example, in biomembranes or on cell cortex, the surface itself may be moving in an uncontrolled way. Scanning perpendicularly to the surface makes it possible to eliminate these motions in the data analysis.
- *Complex motion*. The molecular motion is more complex, possibly a combination of diffusion and flow with static features, or multicomponent or anomalous diffusion. Choose a scan path in combination with spatiotemporal correlation analysis that can reveal complex motion patterns.
- *Parallel measurement*. Need to measure simultaneously at more locations? It may be possible to choose a scan path that passes through all these locations, and the subsequent data analysis produces separate results for each position.

the statistical accuracy for slowly moving molecules and leads to shorter measurement times; short residence times in the detection volume reduce the effect of photobleaching; and the scan speed can be determined with high accuracy, eliminating the need for calibrating the detection volume. The application of sFCS is especially beneficial in measurements on biological membranes where diffusion is usually very slow. Here, an alternative implementation of a moving detection volume has proven very useful: choosing a scan path that is perpendicular to the membrane plane eliminates the effect of membrane movements and instabilities (Ries and Schwille, 2006).

In the following, we describe experimental steps to perform sFCS measurements (see also Box 2) and discuss applications and limitations. We start with a general description of the common features of sFCS. Then we will discuss specific implementations (circular sFCS and line sFCS with a perpendicular scan path) in detail and present their applications.

2. Implementation

sFCS is typically performed on a confocal laser scanning microscope (CLSM) where the sample can be imaged before the scan path is chosen, and which makes it possible to scan the measurement volume during the actual scanning fluorescence correlation spectroscopy (sFCS) measurement across the sample in a user-defined way. The CLSM determines what scan paths can be used. While linear paths of any length and angle are typically possible

Box 2 How to proceed

1. Choose the scan path based on the motivation for using sFCS, and the scan parameters depending on the speed of molecular motion, sample size, etc.
2. *Perform the measurement.* Ideally, the full raw data (photon arrival times) are saved, and the correlation is calculated by the analysis software.
3. *Calculate the correlation*. The algorithm in general depends on the scan path, and some preprocessing may be necessary, for example, due to a moving membrane when measuring diffusion within unsupported membranes.
4. Apply corrections for photobleaching and other irregularities, if necessary.
5. Fit the data with a model dependent on the scan path, and obtain the desired parameters.

with available commercial instruments, circular paths can usually be realized only with homebuilt setups.

Apart from the possibility to scan the measurement volume, the technical requirements for sFCS are identical with those of standard FCS. The main points making a CLSM capable of FCS measurements are briefly summarized in the following paragraphs, while details are extensively described in the literature (Petrov and Schwille, 2008).

The critical parameter for a successful FCS measurement is the size and shape of the measurement volume. This is determined by the focusing of the excitation laser beam, and by the detection geometry of the emission signal. The water immersion objective used should have high numerical aperture to produce a small focus and collect a maximum signal, and a correction collar that allows adjustment for different coverslip thicknesses. Exact positioning of the correction collar yields an undistorted focus, a crucial requirement for any FCS measurement. On the detection side, the confocal pinhole should be adjustable, in both its size and its lateral (ideally also axial) position. The pinhole is not necessary if two-photon excitation is employed.

Another important element is the detector. The standard is an avalanche photodiode, a photon counting detector with high quantum efficiency. Other important parameters of the detector are low dark count (few hundreds of counts per second or less) and weak afterpulsing (ideally of low amplitude and short decay, microseconds or less). The same detector can be used for photon counting imaging, which is becoming increasingly common nowadays in lowlight, single molecule, and quantitative imaging applications (Becker *et al.*, 2004).

The signal from the detector consisting of pulses for each detected photon is processed by the computer. It is desirable to store the whole raw data, that is, the arrival times of all photons, with sufficiently high temporal resolution. This gives the user maximal freedom in the subsequent data analysis. Hardware correlators are practical for alignment and monitoring purposes because they provide the autocorrelation in real time, but should be used in sFCS only together with other means for obtaining the raw fluorescence signal.

Commercial laser scanning microscope systems that provide FCS capability include Confocor 3 with LSM-510 or LSM-710 microscopes (Zeiss, Jena, Germany), TCS SMD FCS (Leica, Wetzlar, Germany), DCS-120 Confocal FLIM system (Becker & Hickl, Berlin, Germany), and Micro Time 200 (Picoquant, Berlin, Germany). The latter two companies also provide all hardware necessary for an implementation of FCS and sFCS in an existing, either commercial or homebuilt, confocal scanning microscope. LSM-710 (Zeiss) is available with an implemented raster image correlation spectroscopy (RICS, see below) option, a type of sFCS.

2.1. Scan paths

The choice of the scan path depends on several factors, mainly on the type of molecular motion motivating the use of sFCS, the sample size and shape, and the options provided by the instrument. All the scan paths considered here lie within the focal plane (do not move to different z positions) and are realized by scanning the laser beam, not the sample stage, which would not be possible to realize at sufficient speed.

The scan paths can be divided into two groups: linear and circular. This division is to some extent due to practical reasons. Line scans can be easily performed with commercial CLSMs. Although the commercial scanning microscopes equipped with galvanometer scanners are also capable of circular scans, this option is usually not software-implemented. The user is limited to homebuilt instruments where the scan path can be controlled with full flexibility.

The circular path with large radius is more or less equivalent to a linear path, and what is said about one is mostly valid for the other. The only difference is in the calculation of the correlation. With the linear path, the termination of the line and possible changes of direction in case of bidirectional scanning have to be taken into account. With the circular path, all points along the circle are equivalent; therefore, no presorting of the data stream is necessary, simplifying the calculation of the autocorrelation. Additionally, circular scans can be faster than linear scans and feature more constant scanning velocities since they require no rapid acceleration.

The most relevant differences between the line and circle scans can be found in the double-line scan, which would be difficult to realize in a circular configuration, and in a small-circle scan, which does not have a line equivalent.

In the following, we briefly describe each scan path and its main area of application (see also Table 15.1).

2.1.1. Single-line and large-circle scans

Large-range scans are typically applied in the following situations: when the molecules move slowly and averaging over a larger population is desired, when spatiotemporal correlation of the molecular motion is of interest, or when we wish to perform correlation analysis at many locations along a line simultaneously. By large range we mean scan path lengths many times larger than the linear dimension of the measurement volume.

When the molecules move slowly, the FCS measurement at one position suffers from poor statistics, because insufficient numbers of molecules pass through the measurement volume during the measurement time (Tcherniak *et al.*, 2009). This results in low accuracy of the fluorescence correlation especially at long correlation times, affecting the values of recovered parameters (diffusion time and particle number). By scanning the focused excitation beam, the measurement is effectively performed at many locations, their number approximately given by the ratio between the length of the scan path and the size of the volume, thus improving the signal-to-noise ratio.

The fluorescence autocorrelation in standard FCS describes the temporal dynamics of molecules leaving the measurement volume. Spatiotemporal correlation curves additionally contain information about the spatial spreading of the molecules from their original location. This additional information is needed to characterize more complex motion than simple diffusion, such as

Table 15.1 Scan paths and their properties

Scan type	Main benefit/application	References
No scanning	Fast diffusion, simple implementation, inhomogeneous sample	Rigler and Elson (2001)
Single-line, large-circle	Slow motion, photobleaching, robustness, spatiotemporal correlation	Petrášek *et al.* (2008b) and Ries *et al.* (2009a)
Small-circle	Robustness, precision, small area	Skinner *et al.* (2005) and Petrášek and Schwille (2008b)
Double-line	Robustness, precision, membrane motion	Ries and Schwille (2006)
Raster	Slow motion, spatiotemporal correlation	Digman *et al.* (2005)
Perpendicular to membrane	Membrane motion	Ries and Schwille (2006)

multicomponent diffusion, combination with flow, reaction kinetics, or anomalous diffusion. This has been exploited in spatiotemporal image correlation spectroscopy (STICS), a type of correlation analysis applied to a sequence of images (Hebert *et al.*, 2005). sFCS also gives us access to spatiotemporal correlation, as described below. Although sFCS features only one spatial dimension (along the scan path), it has higher temporal resolution than STICS, enabling studies of faster processes.

Additionally, the knowledge of spatiotemporal correlation makes it possible to determine from one experiment the diffusion coefficient D and the size of the measurement volume w_0. In standard FCS, these two parameters are combined in the diffusion time $\tau_D = w_0^2/4D$, and to calculate D, the volume size has to be determined in an independent measurement with a molecule of a known diffusion coefficient. The effect of possible optical distortions, which can invalidate this calibration in standard FCS, is avoided in sFCS, because the volume size is determined independently from the fit. The spatial calibration of the scan path is determined by the instrument only, can be performed relatively easily, and is generally not affected by the optical properties of the sample.

Another useful feature of long scan paths is the reduction of the probability that any observed molecule will be photobleached. Due to the motion of the focused laser beam, the total light dose is distributed over a larger area, and the residence time of individual molecules within the focus is reduced. This lowers the chance of photobleaching compared to situations where the slow-moving molecule diffuses through a stationary focus (Petrášek and Schwille, 2008a; Ries *et al.*, 2009a; Satsoura *et al.*, 2007).

When we are interested in correlation analysis at more positions but cannot perform the measurements sequentially, for example, because the sample changes in time, sFCS can be used to perform the measurements in a semi-parallel way. The scan path is chosen so that the beam passes through all the points of interest, the raw data (fluorescence signal) are then sorted depending on the position, and the data from each position are correlated, producing autocorrelation curves at each location. The sorting of the raw data requires that the relation between the fluorescence signal and the position at which it was recorded is known.

The size and shape of the scan path is largely governed by the sample. With the exception of the application described in the last paragraph, the sample should be homogeneous along the scan path, since the obtained results represent an average over the measured area. Generally, larger scan paths are preferable due to better averaging.

2.1.2. Small-circle scan

Circular paths with a radius comparable to the size of the measurement volume are suitable for robust and accurate measurements of diffusion coefficients in situations when the size of the probed volume is not

known or can be affected by the sample (Petrášek and Schwille, 2008b). The principle is the same as with other correlation methods where spatiotemporal correlation is measured: by introducing another spatial measure (scan radius (Petrášek and Schwille, 2008b), distance covered per unit time (Ries *et al.*, 2009a), distance between two foci (Dertinger *et al.*, 2007)), the diffusion coefficient and the volume size in the model function become decoupled and can be determined independently from the fit, resulting in robustness to optical distortions. Small-circle scan is optimal for this purpose: since the radius is small, the correlation values at all lag times are nonzero, and therefore carry useful information, unlike the large-circle scan, where the correlation values outside the narrow peaks are zero (Fig. 15.2). Another important feature is that the scan with a small radius covers a minimal area, meaning that the measurements can be performed also on samples without large homogeneous areas, as is typical in cells.

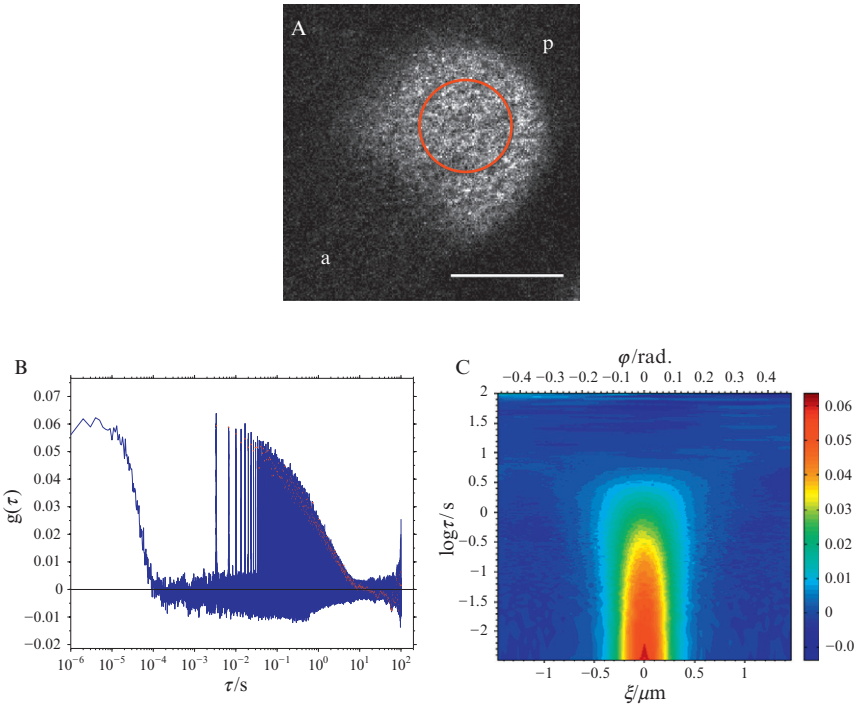

Figure 15.2 Large-circle sFCS in a C. elegans embryo. (A) The laser beam is scanned in a circle on the flat part of the posterior (p) cortex of the embryo where GFP::PAR-2 localizes; the anterior half (a) is without PAR-2. (B) The autocorrelation of the fluorescence signal consists of peaks spaced by the scan period $1/f$ with their amplitude decreasing as in standard FCS. (C) The spatiotemporal correlation of the same signal shows additionally the lateral spreading of the GFP-labeled molecules.

2.1.3. Double-line scan

An alternative way to reach the same goal as described in the previous paragraph is to use double-line scan, whereby two parallel lines separated by a known distance comparable to the measurement volume size are scanned sequentially. Spatial cross-correlation of the signal between the two lines is then used to determine the diffusion coefficient without the need to know the volume size (Chiantia *et al.*, 2006; Ries and Schwille, 2006).

2.1.4. Raster scan

Combination of line scans offset in a perpendicular direction results in a raster scan, commonly used for imaging in laser scanning microscopes. Correlation of raster scan data is the basis of raster image correlation microscopy (RICS) (Digman *et al.*, 2005). In RICS, the correlation of the signal is performed along the scan line and in the direction perpendicular to the scan line, giving access to two different temporal scales. Raster correlation is closely related to image correlation spectroscopy, which is described elsewhere (Wiseman *et al.*, 2000).

2.1.5. sFCS with membrane motion

When molecules diffuse within a membrane, or another two-dimensional structure, and the membrane moves, due to undulations, cell growth or dynamics, or other reasons, the standard FCS faces the problem that the autocorrelation function contains the contributions of both, molecular and membrane motion, which cannot be easily separated. The solution by means of sFCS is to scan the laser focus in a line perpendicular to the fluctuating membrane surface and to correlate the intensities from subsequent passages of the beam through the membrane. Only the signal from around the maximum in each scan line is correlated, regardless of where this maximum occurred, thus eliminating any effects of membrane motion (Fig. 15.4). The temporal resolution in this case is limited to the scan period; this is, however, often sufficient due to relatively slow motion of molecules in membranes.

This approach can be combined with a double-line scan described above, thus gaining the advantage of robustness against optical distortions (Fig. 15.5).

2.2. Calibration of the scan path

Many of the implementations of sFCS rely on the exact calibration of the scan path. In circular scan methods, the scan radius must be known; in double-line and double-focus approaches the knowledge of the distance between the two scanned lines is required; and with a single-line scan, the scan speed is important. These dimensions can be determined in the slow

scan limit by imaging a calibration standard, for example, a Ronchi ruling, a stripe pattern with well-defined spacing. This calibration need not be valid at high scan speeds, since the actual response of the scanning device to the driving commands may vary. Then a "dynamic calibration" is required, whereby the same scan parameters as during the measurement are used. In the small-circle scan method and the line-scan method, the dynamic calibration can be performed by analyzing the signal reflected from the Ronchi ruling at high scan frequencies (Petrášek and Schwille, 2008b; Ries *et al.*, 2009a). Another possibility is to use the sensor signal from the scanners (if available) to determine the exact scanner position. The distance between two lines can be determined by scanning over a film of immobilized fluorophores. The bleached traces are then analyzed in a high-resolution LSM image by fitting the profiles with a double-Gaussian (Ries and Schwille, 2006).

3. Data Analysis

Data analysis in sFCS can be roughly divided into three steps: calculation of the correlation from the raw data, application of corrections, and fitting of the data to extract the parameters of interest. These steps are described in more detail in the following sections.

3.1. Calculation of correlation curves

The correlation $g_{12}(\tau)$ of the fluorescence signals $F_1(t)$ and $F_2(t)$ is defined in the following way:

$$g_{12}(\tau) = \frac{\langle \delta F_1(t) \delta F_2(t+\tau) \rangle}{\langle F_1(t) \rangle \langle F_2(t) \rangle}, \tag{15.1}$$

where $\langle F_1(t) \rangle$ and $\langle F_2(t) \rangle$ are the averages of $F_1(t)$ and $F_2(t)$, and $\delta F_1(t) = F_1(t) - \langle F_1(t) \rangle$, $\delta F_2(t) = F_2(t) - \langle F_2(t) \rangle$. The signals $F_1(t)$and $F_2(t)$ can be equal, in which case Eq. (15.1) gives the autocorrelation $g(\tau)$ of $F(t) = F_1(t) = F_2(t)$. Alternatively, the two signals can originate from two different spatial channels, giving spatial cross-correlation, or from two different spectral channels, as in dual-color versions of FCS, yielding spectral cross-correlation (see Box 3).

Due to the variability of scan paths and goals in sFCS, several different ways of calculating the correlation from Eq. (15.1) are employed, in contrast to standard FCS, where the autocorrelation is either directly provided by the hardware correlator, or calculated by a multiple-tau method (Schätzel, 1990).

Box 3 Dual-color cross-correlation spectroscopy

To measure binding between two distinctly labeled molecules, dual-color fluorescence cross-correlation spectroscopy (FCCS) (Schwille *et al.*, 1997) can be employed. Here, two spectral channels are used to calculate the autocorrelation curves and also the spectral cross-correlation curve. Only if the two binding partners diffuse as an entity, do they give rise to a significant cross-correlation amplitude that can then be used to study the degree of binding. Dual-color cross-correlation can be used in general with all implementations of sFCS discussed here if two spectral channels are used.

Under the assumption that the red and green detection areas are equal in size and completely overlapping, we can calculate the relative binding from the amplitudes of the autocorrelation curves $G_r(0)$ and $G_g(0)$ and the cross-correlation amplitude $G_{rg}(0)$:

$$\frac{C_{rg}}{C_{rg}+C_g}=\frac{G_{rg}(0)}{G_r(0)},\quad \frac{C_{rg}}{C_{rg}+C_r}=\frac{G_{rg}(0)}{G_g(0)}, \tag{15.13}$$

where C_g, C_r and C_{rg} are the concentration of green-labelled, red-labelled and double-labelled molecules, respectively.

Overlapping emission spectra and spectral cross talk, usually from the green fluorophore into the red channel, introduces additional similarities between the fluorescence fluctuations in the two channels and can therefore result in a false-positive cross-correlation. Spectral cross talk can be avoided by using alternating excitation (Muller *et al.*, 2005; Thews *et al.*, 2005) or has to be taken into account during data analysis (Rička and Binkert, 1989).

In the case of scanning FCCS spatial heterogeneities can also induce a false-positive cross-correlation. Correction schemes for heterogeneities must be explicitly tested on negative controls to avoid this artifact.

The multiple-tau method takes advantage of the fact that autocorrelations typically encountered in FCS decay progressively slower at longer lag times τ, that is, the longer the lag time, the smaller the change in the correlation value. The correlation is calculated at time intervals and bin widths increasing with the lag time, rather than at fixed intervals with fixed bin width. Since typical correlations span time periods of many orders of magnitude, the number of lag times at which the correlation is evaluated is greatly reduced without losing much information. In commonly used implementations of the multiple-tau method the lag channel width and interval are doubled every m channels, where m is usually 8, 16, or more. The algorithms for the

calculation of $g(\tau)$ from the sequence of the photon arrival times are described in detail elsewhere (Magatti and Ferri, 2003; Schätzel, 1990).

In sFCS with a circular path, the periodic motion introduces modulations to the correlation of the fluorescence signal. When the molecular motion is slow, the periodic modulation persists even at long correlation times, and may be averaged out by the wide bins in the multiple-tau method. Sometimes, it is sufficient to increase the number of constant-width channels m to 32, 64, or more in the multiple-tau method to refine the sampling (Petrášek and Schwille, 2008b), in other cases linear correlation with constant channel width has to be used (Petrášek *et al.*, 2008b).

The term "linear correlation" refers to the correlation calculated at lag times τ spaced equally in time and with equal bin width. The direct calculation from the definition in Eq. (15.1) is computationally too intensive, due to the high number of correlation channels τ_i and real-time channels t_i over which the averages in Eq. (15.1) are calculated. The standard way is therefore to exploit the relationship between the autocorrelation and the Fourier transform of $F(t)$ together with the efficient algorithms for Fourier transform calculation. A possible problem may be the size of high-resolution data sets compared to the available computer memory. In such cases, a solution with an intermediate disk storage for large data files has been described (Petrášek *et al.*, 2008a).

In sFCS methods with the linear scan path, one typically sorts the raw data first, depending on the position from which the signal originates. To do this, the relationship between the signal and the measurement volume position has to be known at all times. The fluorescence is then a function of both the position $\mathbf{r}$ and the time t: $F(\mathbf{r}, t)$, and a spatiotemporal correlation $g(\xi, \tau)$ can be defined as

$$g(\xi, \tau) = \frac{\langle \delta F(\mathbf{r}, t) \delta F(\mathbf{r} + \xi, t + \tau) \rangle}{\langle F(t) \rangle^2}. \tag{15.2}$$

A spatiotemporal cross-correlation for two different signals can be defined in a way analogous to Eq. (15.1). The spatiotemporal correlation is calculated either by using the linear correlation method for both time and space or by combining the multiple-tau correlation for time and the linear correlation for space.

In applications where sFCS is used to perform measurements at multiple locations simultaneously only temporal correlation at desired positions $\mathbf{r}_i$ is calculated from the appropriate parts of the raw data $F(\mathbf{r}_i, t)$.

In the application of sFCS to molecules in fluctuating membranes, the spatial resolution of $F(\mathbf{r}, t)$ is used to select only the part of the signal originating from the membrane and only temporal correlation is performed. This principle allows the elimination of membrane motion from the temporal correlation, and is described in more detail in Section 4.

3.2. Corrections

The correlation calculated from the raw data often does not only represent the studied molecules but may be influenced by other factors, such as fluorescence background, gradual fluorophore depletion due to photobleaching, unspecific long-term fluctuations, etc. Here we describe how these effects can be corrected for before the correlation is fitted with a theoretical model.

3.2.1. Fluorescent background

The signal background is often caused by the autofluorescence of native sample structures, but can also originate from optical components of the instrument, or poor blocking of Raman scattering. The background may be constant and uncorrelated in time, or exhibit an autocorrelation if it comes from diffusing molecules. It can be either uniform in space or vary as the scanning beam passes through different structures.

The effect of a constant background is rescaling of the amplitude of the autocorrelation $g(\tau)$ and can be corrected for if the background value B can be determined independently:

$$g_c(\tau) = \left(\frac{\langle F\rangle}{\langle F\rangle - B}\right)^2 g(\tau). \tag{15.3}$$

If the background $B(t)$ is correlated in time and can be measured independently from, for example, a control sample without fluorescence labeling, then the correlation of $B(t)$ can be incorporated into the analysis as a fixed second component in a two-component fit (Rigler and Elson, 2001).

3.2.2. Photobleaching

Photobleaching—the irreversible photochemical destruction of a fluorophore—leads to two kinds of artifacts on different timescales. (1)The sudden disappearance of a fluorophore results in shorter residence times in the detection volume and apparent faster diffusion. (2) Measurements within a closed small volume, for example, a cell or a vesicle, can lead to a gradual fluorescence depletion due to photobleaching. The same effect is encountered in two-dimensional systems, such as membranes, where the fluorophore depletion is not sufficiently compensated by influx of fresh molecules through diffusion. Under these conditions, the system is no longer in a steady state and correlation curves are seriously distorted.

To avoid the first artifact—photobleaching in the detection volume—the excitation laser power has to be reduced until only a negligible fraction of fluorophores is bleached. It is advisable to determine the onset of photobleaching with an intensity series.

The second artifact—depletion of fluorophores around the detection area due to photobleaching—is more difficult to avoid, since it can play a

role even for minimal excitation laser powers, especially if high concentrations are used. To correct for depletion (Ries *et al.*, 2009a), the slow decay of the intensity trace $F(t)$ is first approximated by an analytical function $b(t)$. For a restricted reservoir, the decay can be assumed to be exponential: $b(t) = b_0 \, e^{-t/t_b}$. If depletion is due to the limited geometry in membrane measurements or the reservoir is connected weakly to a larger reservoir, a multiexponential is a good choice, and often two exponentials are sufficient. With the knowledge of $b(t)$, the intensity trace can be corrected in the following way prior to calculating correlation curves:

$$F_c(t) = \frac{F(t)}{\sqrt{b(t)/b(0)}} + b(0)\left(1 - \sqrt{b(t)/b(0)}\right). \tag{15.4}$$

This transformation leads to a constant mean value and constant fluctuations with time, not distinguishable from a system in a steady state. The correlation curve calculated from the corrected intensity trace $F_c(t)$ is no longer distorted by the decaying intensity and the concentration inferred by fitting is the initial concentration. Note that this approach does not correct for the apparent reduction of the concentration and diffusion time due to bleaching in the detection volume as described in the previous paragraph.

3.2.3. Spatial heterogeneities

In sFCS, the beam passes through different parts of the sample, potentially crossing brighter or darker static structures or regions with varying background. This can lead to periodic oscillations in the correlation curve, or to longtime distortions. Similar distortions may be present at long correlation times, due to poor statistics. Although these effects cannot be removed by an independent measurement on a control sample, as with constant background described above, it is still desirable to eliminate these distortions to be able to better fit the data. One way to filter out these unwanted fluctuations from the correlation curve is to assume that the measured fluorescence intensity $F(t)$ can be written as

$$F(t) = f(t)h(t), \tag{15.5}$$

where $f(t)$ is the "pure" signal and $h(t)$ is a modulation function reflecting either the periodic signal modulation along the scan path or long-term fluctuations in $F(t)$. In case of no distortions, $h(t) = 1$. The modulation function $h(t)$ can be determined either by smoothing the raw data with a user-defined bin width or by fitting the raw data with an analytical function, as described above for the depletion case.

It follows from the definition of the correlation function that the desired autocorrelation $g_c(\tau)$ of $f(t)$ is related to the autocorrelation $g(\tau)$ of $F(t)$ and the autocorrelation $g_h(\tau)$ of $h(t)$ in the following way:

$$g_c(\tau) = (g(\tau) + 1)/(g_h(\tau) + 1) - 1. \tag{15.6}$$

Care should be taken with the choice of the bin width when calculating $h(t)$, since this correction filters out all fluctuations on the longer timescale, without discriminating between the "true" signal and the interfering background. The correction of Eq. (15.6) remains approximately valid if the modulation by $h(t)$ is not multiplicative as in Eq. (15.5), but additive, and if $h(t)$ is small compared to $f(t)$.

The filtering using Eq. (15.6) affects only the temporal correlation profile, but does not correct the amplitude. This is because the value of the amplitude depends on the nature of the fluctuations (their variance). If the nature of the fluctuations is known throughout the measurement, the amplitude can also be corrected. For example, in the case of photodepletion as described above, the temporal profile can be corrected by Eq. (15.6) with $h(t) = b(t)/b(0)$. The variance of the particle number changes as the concentration decreases, and it can be shown that the correct amplitude can be obtained by dividing $g_c(\tau)$ by $\langle b(0)/b(t)\rangle$.

It is also possible to use the effects of the static structures on the autocorrelation to identify immobilized particles, rather than to filter this information out, as implemented in one form of small-circle sFCS (Skinner *et al.*, 2005).

It should be stressed that all corrections described here are not specific to sFCS but are applicable to standard FCS as well.

3.3. Data fitting

3.3.1. Fitting models

Scanning affects the fluctuations of the measured signal, therefore it is only natural that it becomes visually apparent in the calculated autocorrelation, and also has to be included in the fitting models. Since the parameters of the scan are known, scanning does not increase the number of fitting parameters that might lead to less stable or undetermined fits. To the contrary, sFCS correlations contain more information, making some of the fitting parameters less correlated and the fits more stable.

In the absence of scanning the model function $G_0(\tau)$ for free diffusion in three dimensions is

$$G_0(\tau) = \frac{1}{c}\underbrace{\frac{1}{\sqrt{\pi}w_0}\left(1+\frac{\tau}{\tau_D}\right)^{-1/2}}_{x}\underbrace{\frac{1}{\sqrt{\pi}w_0}\left(1+\frac{\tau}{\tau_D}\right)^{-1/2}}_{y}\underbrace{\frac{1}{\sqrt{\pi}w_0 S}\left(1+\frac{\tau}{\tau_D S^2}\right)^{-1/2}}_{z}, \tag{15.7}$$

where c is the concentration, w_0 the lateral size of the measurement volume, $w_0 S$ its axial size, and $\tau_D = w_0^2/(4D)$ the diffusion time. The equation has been purposefully divided into three terms, each corresponding to diffusion along one dimension. If the molecular motion is restricted to two dimensions, for example, to a vertical yz or horizontal xy plane, only the corresponding terms remain. Here we use the capital symbol $G(\tau)$ for models while the lowercase $g(\tau)$ is reserved for correlations calculated from the data.

Many organic dyes and fluorescent proteins exhibit fast, approximately exponential dynamics at sub-ms timescales. The origins of these fluctuations are singlet–triplet transitions, protonation reactions, etc. They are usually taken into account by introducing a multiplicative term into Eq. (15.7):

$$G'_0(\tau) = G_0(\tau)\frac{1 - T + T\,\mathrm{e}^{-\tau/\tau_T}}{1 - T}, \tag{15.8}$$

where T is the fraction of the molecules in the dark (triplet, protonated) state, and τ_T is the characteristic relaxation time. The phenomena investigated with sFCS often occur on considerably longer timescales, therefore the fast dynamics term can usually be omitted.

To see how the beam motion enters the models it is advantageous to start with the model for a circular scan:

$$G(\tau) = G_0(\tau)\exp\left(-\frac{4R^2\sin^2(\omega\tau/2)}{w_0^2(1+\tau/\tau_D)}\right). \tag{15.9}$$

The autocorrelation function with a fixed measurement volume is multiplied by a scan factor that depends on the scan frequency ω and the radius R, both of which are known. Additionally, the scan factor depends on the diffusion coefficient D via τ_D and beam size w_0 in a way that decouples these two parameters, making it possible to determine each of them independently from one fit. This decoupling is the basis of the precision and robustness of both circle- and line-scan methods.

The autocorrelation for a linear scan with velocity v follows from Eq. (15.9) by assuming the limit of large radius, $R \to \infty$, while maintaining the constant velocity $v = R\omega$:

$$G(\tau) = G_0(\tau)\exp\left(-\frac{v^2\tau^2}{w_0^2(1+\tau/\tau_D)}\right). \tag{15.10}$$

The spatiotemporal correlation $G(\xi, \tau)$ for a linear scan follows directly from Eq. (15.10) by substituting $\xi = v\,\tau$:

$$G(\xi,\tau) = G_0(\tau)\exp\left(-\frac{\xi^2}{w_0^2(1+\tau/\tau_D)}\right). \tag{15.11}$$

This equation at the same time represents a cross-correlation between two volumes separated by the distance $d \equiv \xi$. In practice, the sFCS measurement does not provide us with the spatiotemporal correlation at all values of ξ and τ, but only at a subset of these. With a linear scan, the correlation is obtained at points where $\tau = \xi/v + nT$, where T is the scan period. In case of the circular scan, it is obtained at points where $\xi = 2R\sin(\omega\tau/2)$.

3.3.2. Fitting

The calculated and corrected correlation is fitted to the model using standard nonlinear, least squares fitting procedures as implemented in common data analysis software (Matlab, Origin, etc.). The results of the fit are the optimal parameter values that minimize the difference between the model and the data. We recommend to use weighting of the data points to achieve fits unbiased toward noisier data points. The weights w_i are usually estimated from the correlations by comparing the variations between $n = 2k + 1$ data points surrounding the data point $g_i : g_{i-k}, \ldots, g_{i+k}$. The weight w_i is then taken as the inverse value of the standard deviation of these n points. A problem may arise when the deviation between the neighboring data points is not only due to random noise but due to abrupt variations of the correlation g_i, as can happen with correlations modulated by the periodic scanning motion. The weights in these regions are then underestimated. In this case, the weights can be estimated from residuals of a preliminary unweighted fit, or the weights can be approximated by a smooth function, thus eliminating the bias at points of large variation.

4. Applications

In this section, we describe several applications of sFCS, explaining the motivation behind using sFCS instead of standard (fixed-focus) FCS, the choice of the particular scan path, the details of implementation and analysis not mentioned already in the general part above, and the results obtained, demonstrating the advantages of the various sFCS approaches.

4.1. sFCS in *Caenorhabditis elegans* embryo

We have applied circular sFCS with large-circle diameter to the investigation of PAR-2 protein dynamics on the cortex of living *Caenorhabditis elegans* embryo in the first division stage (Petrášek *et al.*, 2008a,b). Several problems prevented us from using standard FCS in this case: the cortex does not stay in the same position for a sufficiently long time, the molecules move very slowly making it impossible to obtain good statistics within the

measurement time window limited by embryo development, and the slow motion causes photobleaching artifacts to be overwhelming.

To circumvent these problems, we focused onto the bottom part of the embryo where a large part of the cortex is flattened and steady due to contact with the coverslip. Then we chose the largest circular scan path that still lies within the posterior half of the embryo and along which the fluorescence intensity is uniform (Fig. 15.2A). It would also be possible to use a linear scan; however, the length of the circle perimeter is larger than any line that would fit within the fluorescent part of the embryo, resulting in better averaging. Additionally, the data processing of the circle-scan data is more straightforward and no time is wasted due to the laser fly back and turning points as in the line scan. Scanning the beam practically eliminates the problems with photobleaching, because the total light dose is distributed along the whole scan path.

Figure 15.2B shows the measured autocorrelation. The maxima of the uniformly spaced peaks correspond to a common autocorrelation as known from standard FCS. The peak spacing is determined by the scan frequency, 300 Hz in this case, a value close to the maximum technically possible with the setup used. A larger scan frequency would increase the temporal resolution at short correlation times. The better averaging achieved by probing many locations along the scan path results in meaningful correlation values up to the range of 1–10 s, which is not achievable with standard FCS within the measurement time of 100 s.

More information than available from the amplitude of the correlation peaks shown in Fig. 15.2B can be obtained by replotting the data as a spatiotemporal correlation (Fig. 15.2C). Spatial information is contained in the shape of the peaks and is obtained by converting the correlation time into the spatial correlation coordinate$\xi : \xi = 2R \sin(\pi f \tau)$. This spatial correlation contains information about lateral spreading, and, in principle, makes it possible to distinguish lateral motion from detachment of proteins from the cortex. An analysis of the spatiotemporal correlation data shows that the best description requires a model with at least two diffusion components.

These experiments have been performed using two-photon excitation, which has the benefit of reduced photobleaching in the embryo as a whole, since the molecules outside the focal volume are not excited. Additionally, no signs of phototoxicity are observed. Taken together, these two features of two-photon excitation enable long observation times, permitting monitoring of embryo development.

4.2. Small-circle sFCS

sFCS with a small circular path is a convenient way to measure spatiotemporal correlations within a minimum sample volume. In its original application (Skinner *et al.*, 2005), it was implemented as position-sensitive

correlation, which allows determination of not only diffusion, but also direction and magnitude of flow, immobilization, and any combination of these. We have applied a simpler analysis, without the position sensitivity, and used the spatial information encoded in the correlation to determine the diffusion coefficients in a precise and robust way, even in the presence of optical distortions and photobleaching (Petrášek and Schwille, 2008b).

When the beam is scanned in a small circle (Fig. 15.3A), the autocorrelation is modulated as a result of scanning (Fig. 15.3B), but contrary to the large-circle scan, the width of the peaks at multiples of the scan period is comparable to their spacing. In both cases, the model autocorrelation is expressed by Eq. (15.9). This modulation makes it possible to determine

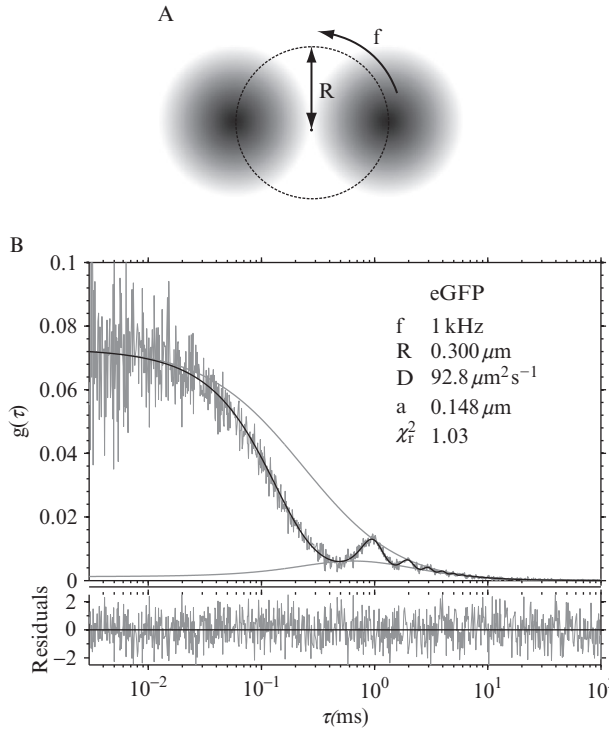

Figure 15.3 Small-circle sFCS for robust and precise determination of diffusion coefficients. (A) The laser beam is scanned in a circle with frequency f and radius R which is comparable to the measurement volume size w_0. (B) The autocorrelation of the fluorescence signal is modulated as a result of scanning. The upper and lower envelopes correspond to the autocorrelation at a fixed position and the spatial cross-correlation at a distance equal to the diameter $2R$ of the scanned circle, respectively. From a fit of the data with Eq. (15.9) the diffusion coefficient D and the volume size $w_0 = 2a$ are determined. The sample is eGFP (enhanced Green Fluorescent Protein) in buffer solution.

both the diffusion coefficient D and the volume size w_0 independently. The upper envelope of the oscillating autocorrelation is the curve that would be measured with standard FCS. The lower envelope corresponds to a spatial cross-correlation between two extreme positions of the moving laser focus, that is, at a distance $2R$, as shown in Fig. 15.3A.

The choice of the scan frequency f will typically be limited by the instrument and often has such a value that the scan period $1/f$ is longer than the diffusion time τ_D of the investigated molecules. The optimal scan radius R was shown to lie near the value of $0.5w_0\sqrt{2+1/(f\tau_D)}$, which is comparable to the measurement volume size w_0. The optimal scan radius approximately corresponds to the situation where the first maximum of the autocorrelation at the time $1/f$ coincides with the maximum of the cross-correlation forming the lower envelope of the scanning autocorrelation (Fig. 15.3B).

This implementation of sFCS, apart from yielding the diffusion coefficient without any knowledge of the volume size w_0, was shown to be more robust than standard FCS against photobleaching and optical distortions that change the volume size. Its potential has been demonstrated both in solutions and in living cells.

4.3. sFCS with a perpendicular scan path to measure in unstable membranes

For measurements in biological membranes, membrane movements or instabilities can be a major problem. Considering the lateral and axial sizes of the focal spot of $\approx$250 and $\approx$700 nm, respectively, shifts as small as 100 nm during a measurement time of several minutes are already devastating and lead to strong distortions of the correlation curves. The choice of a scan path that is perpendicular to the membrane plane avoids this problem as the detection volume crosses the membrane in a reproducible way independently of membrane movements. This method was first introduced with a circular scan path to measure membrane dynamics in presence of a strong background in solution (Ruan *et al.*, 2004). Here we concentrate on the implementation with a linear scan path (Ries and Schwille, 2006), since it can be readily used with a commercial laser scanning microscope. In addition, it can be easily extended to dual-focus FCS for exact diffusion measurements without the need for calibrating the detection volume, and to dual-color FCS to measure interactions in membranes.

In this implementation of sFCS, the scan path is chosen in a way that it crosses the vertical membrane perpendicularly (see Fig. 15.4). The intersection of the scan path with the membrane defines the detection area. During data analysis, the intensity fluctuations in this detection area have to be extracted to calculate correlation curves. The necessary steps are as follows:

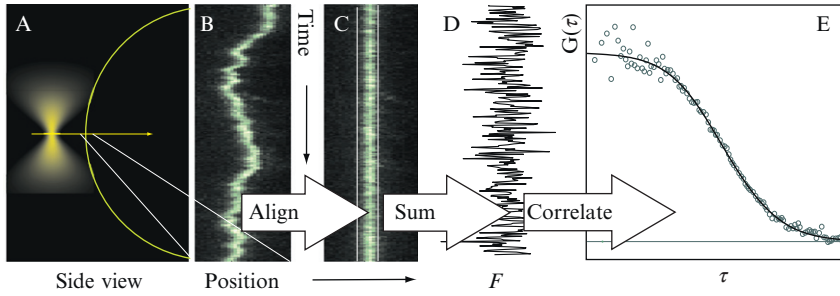

Figure 15.4 *Principle of sFCS with the scan path perpendicular to a membrane.* (A) In sFCS the detection volume is repeatedly scanned perpendicularly through a vertical membrane. The individual line scans can be arranged as a pseudo-image, (B) where the vertical axis denotes the time. In this pseudo-image the membrane is clearly visible. Due to membrane movements, the position of the membrane is not constant in time. These instabilities can be corrected for by shifting each line scan in such a way that the membrane becomes a straight line. (C) For each scan, membrane contributions are added up to give one point in the intensity trace (D) which can then be used to calculate the autocorrelation curve $G(\tau)$ (E).

1. *Construction of pseudo-image*. In case a commercial laser scanning microscope, such as Zeiss LSM-510, is used in the line-scan mode, the raw data will already be in the form of a pseudo-image, where the individual line scans are arranged next to each other. Then the horizontal axis denotes the position in the sample and the vertical axis the time. If the raw data consist of photon arrival times, the reconstruction of the pseudo-image relies on knowledge of the repetition rate. The use of beginning-of-line marker signals, automatically inserted into the data file by the software controlling the scanners, is most accurate. If those are not available, the repetition rate can be determined from the periodicity of the signal (Ries and Schwille, 2006).
2. *Identification of the membrane*. To reduce the background and improve the signal-to-noise ratio, only the signal in a small window around the membrane is used to construct the intensity trace. The position of the membrane at a given time t_i can be determined by evaluating the position of the intensity maximum in an average of several hundred scans around the t_i.
3. *Construction of the fluctuating intensity trace*. Photons collected within a time window Δt around the intensity maximum are summed up to result in the intensity F_i. The time window should be large enough that no signal from the membrane is lost, but small enough to reject most of the background noise. A good choice is to include all photons within $-2\sigma \cdots 2\sigma$ of the Gaussian approximation of the apparent membrane profile.

4. *Calculation of the correlation curve*. The correlation curve can be calculated using a standard multiple-tau correlation algorithm (Magatti and Ferri, 2003).
5. *Data fitting*. The effective detection area is described by a two-dimensional elliptical Gaussian with an aspect ratio of $S = w_z/w_x$. The correlation function describing the experimental correlation curve is given by Eq. (15.7) using only the γ and z parts (Ries and Schwille, 2006). Note that due to the limited time resolution of approximately 1 ms, triplet dynamics need not be included in the model.

A prerequisite for the use of this implementation of sFCS is a vertical membrane. On the length scale of the detection area (1 μm), the curvature should be small. This need for a vertical membrane seems to preclude its application to adherent cells. A solution is to grow cells on glass beads with a diameter of 10–50 μm. Plasma membranes of cells at the equator of the beads are predominantly vertical and are well suited for sFCS.

However, inhomogeneities on the micrometer scale due to protrusions or interactions with the cytoskeleton still limit the applicability of FCS. Plasma membrane spheres (Lingwood *et al.*, 2008) allow the investigation of processes in plasma membranes in a much simpler, spherical geometry which is optimally suited for sFCS. By measuring diffusion coefficients with dual-focus sFCS, we could show that the cross-linking of the lipid GM1 by the protein CTxB leads to a lipid-driven raft-like phase separation in plasma membrane spheres (Lingwood *et al.*, 2008).

4.4. Dual-focus sFCS

To overcome problems caused by optical aberrations, saturation, and other experimental uncertainties that render calibration measurements to determine the size of the detection area inaccurate, dual-focus FCS (Dertinger *et al.*, 2007) can be employed. It employs two spatial detection areas with a well-defined and known distance. Here, the calibration of the detection area is replaced by the determination of this distance, which can be measured more precisely, and, most importantly, is constant for all measurements.

In two-focus sFCS (Fig. 15.5), two parallel lines, spatially offset by a distance d, are scanned through the membrane in an alternating fashion. The intersections with the membrane give rise to two intensity traces $F_1(t)$ and $F_2(t)$, from which the autocorrelation curves $g_1(\tau)$ and $g_2(\tau)$ and also the spatial cross-correlation curves $g_{12}(\tau)$ and $g_{21}(\tau)$ can be calculated using Eq. (15.1).

The model function for the experimental cross-correlation curves in case of free diffusion is given by Eq. (15.7) (γ and z parts) and Eq. (15.11) with $\xi = d$ (Ries and Schwille, 2006):

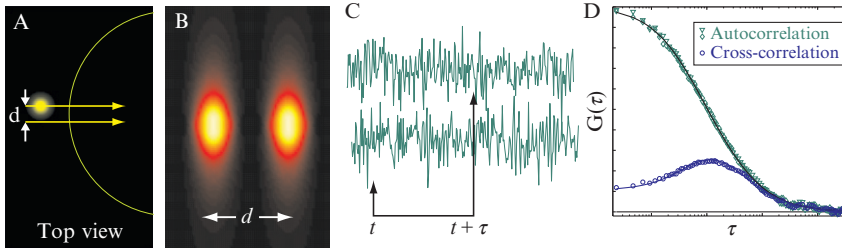

Figure 15.5 Dual-focus sFCS. (A) Two parallel lines are alternatingly scanned in a perpendicular path through the membrane. (B) The intersections with the membrane define two detection areas. From the intensities in the two detection areas (C) the auto- and spatial cross-correlation curves can be calculated. (D) If the distance d between the detection areas is known, a fit of the correlation curves allows direct determination of concentrations and diffusion coefficients without the need for calibrating the size of the detection area.

$$G_{12}(\tau) = G_{21}(\tau) = \frac{1}{c\pi S w_0^2}\left(1+\frac{4D\tau}{w_0^2}\right)^{-1/2}\left(1+\frac{4D\tau}{w_0^2 S^2}\right)^{-1/2} \times \exp\left(-\frac{d^2}{w_0^2+4D\tau}\right). \tag{15.12}$$

Once the distance d is known, the diffusion coefficient D, the concentration c and the waist of the laser focus w_0 can be determined directly by fitting the data with Eq. (15.12) without any additional calibration measurement (Dertinger *et al.*, 2007). The autocorrelation function follows from Eq. (15.12) for $d = 0$.

The photons in the two foci are not collected within the same time window, but with a delay t_d, which is usually given by the scan period. Therefore, the cross-correlation curves are shifted with respect to the autocorrelation curves by this delay time, and this needs to be taken into account during data analysis (Ries and Schwille, 2006).

Two lines can be scanned with commercial laser scanning microscopes by using the frame mode with $N \times 2$ pixels. However, for the maximum repetition rate, the lines are not necessarily parallel. The following settings result in parallel lines in the Zeiss LSM-510: bidirectional multitrack mode, 32×2 pixels per frame, illumination only during the second track.

4.5. Dual-color sFCS

In membranes, binding can be measured with dual-color sFCS using two spectral channels (see Box 3). By scanning every other line with a different color and detecting the photons only in the corresponding channel,

contributions from two different fluorophores can be separated completely and spectral cross talk is avoided (Muller *et al.*, 2005; Ries and Schwille, 2006; Thews *et al.*, 2005). From the two intensity traces, red and green autocorrelation curves and the cross-correlation curve can be calculated. By fitting the correlation curves with Eq. (15.7), their amplitudes can be obtained. The relative binding can then be calculated with Eq. (15.13) below.

We applied dual-color sFCS to study the binding affinities of the apoptotic proteins tBid and Bcl_{XL} in giant unilamellar vesicles, micrometer sized liposomes (García-Sáez *et al.*, 2009). We could show that their interaction is drastically enhanced in the membrane compared to free solution.

The application of sFCS is not limited to single cells, but can be applied to multicellular organisms. In tissue, most cells exhibit large vertical membranes, well suited for sFCS. We combined dual-focus sFCS and dual-color sFCS with conventional static-volume FCS to determine the mobilities and binding affinities of fibroblast growth factor receptors (Fgfr1, Fgfr4) to their extracellular ligand Fgf8 directly in living gastrulating zebra fish embryos. Here, dual-focus sFCS was used to measure the diffusion coefficients of the receptors in the plasma membranes, and the size of the detection area. This internal calibration is very useful due to optical distortions in tissue. Dual-color sFCS with alternating excitation was used to determine the concentrations of the receptors and receptor–ligand complexes in the membrane, whereas static-volume FCS measured the free-ligand concentration in the extracellular space (Ries *et al.*, 2009b). Using global data analysis we could infer the dissociation constants between Fgfr1 or Fgfr4 and Fgf8 and estimate the endogenous receptor concentration.

5. Conclusion

We aimed to present the family of sFCS methods with an eye on the problems they address and the measurement geometries used to implement them (i.e., the scan path). Successful application of sFCS requires understanding of the motivation for using scanning in any given implementation, as well as a knowledge of its limitations. The general aspects of sFCS, including implementation and data analysis, were supplemented by several examples of applications of different sFCS approaches. Altogether, this article should guide the user not only to reproduce an existing sFCS method, but also to modify it or to design a new implementation particularly suited to the problem investigated.

REFERENCES

Bacia, K., and Schwille, P. (2003). A dynamic view of cellular processes by in vivo fluorescence auto-and cross-correlation spectroscopy. *Methods* **29,** 74–85.

Bacia, K., Kim, S., and Schwille, P. (2006). Fluorescence cross-correlation spectroscopy in living cells. *Nat. Methods* **3,** 83–89.

Becker, W., Bergmann, A., Hink, M. A., Konig, K., Benndorf, K., and Biskup, C. (2004). Fluorescence lifetime imaging by time-correlated single-photon counting. *Microsc. Res. Tech.* **63,** 58–66.

Chiantia, S., Ries, J., Kahya, N., and Schwille, P. (2006). Combined AFM and two-focus SFCS study of raft-exhibiting model membranes. *ChemPhysChem* **7,** 2409–2418.

Dertinger, T., Pacheco, V., von der Hocht, I., Hartmann, R., Gregor, I., and Enderlein, J. (2007). Two-focus fluorescence correlation spectroscopy: a new tool for accurate and absolute diffusion measurements. *ChemPhysChem* **8,** 433–443.

Digman, M. A., Brown, C. M., Sengupta, P., Wiseman, P. W., Horwitz, A. R., and Gratton, E. (2005). Measuring fast dynamics in solutions and cells with a laser scanning microscope. *Biophys. J.* **89,** 1317–1327.

Enderlein, J., Gregor, I., Patra, D., Dertinger, T., and Kaupp, U. B. (2005). Performance of fluorescence correlation spectroscopy for measuring diffusion and concentration. *ChemPhysChem* **6,** 2324–2336.

García-Sáez, A. J., Ries, J., Orzáez, M., Pérez-Payà, E., and Schwille, P. (2009). Membrane promotes tBid interaction with Bcl-xL. *Nat. Struct. Mol. Biol.* **16,** 1178–1185.

Hebert, B., Costantino, S., and Wiseman, P. W. (2005). Spatiotemporal image correlation spectroscopy (STICS) theory, verification, and application to protein velocity mapping in living CHO cells. *Biophys. J.* **88,** 3601–3614.

Kim, S. A., Heinze, K. G., and Schwille, P. (2007). Fluorescence correlation spectroscopy in living cells. *Nat. Methods* **4,** 963–973.

Lingwood, D., Ries, J., Schwille, P., and Simons, K. (2008). Plasma membranes are poised for activation of raft phase coalescence at physiological temperature. *Proc. Natl. Acad. Sci. USA* **105,** 10005–10010.

Magatti, D., and Ferri, F. (2003). 25 ns software correlator for photon and fluorescence correlation spectroscopy. *Rev. Sci. Instrum.* **74,** 1135–1144.

Muller, B., Zaychikov, E., Brauchle, C., and Lamb, D. (2005). Pulsed interleaved excitation. *Biophys. J.* **89,** 3508–3522.

Petrášek, Z., and Schwille, P. (2008a). Photobleaching in two-photon scanning fluorescence correlation spectroscopy. *ChemPhysChem* **9,** 147–158.

Petrášek, Z., and Schwille, P. (2008b). Precise measurement of diffusion coefficients using scanning fluorescence correlation spectroscopy. *Biophys. J.* **94,** 1437–1448.

Petrášek, Z., and Schwille, P. (2008c). Scanning fluorescence correlation spectroscopy. *In* ''Single Molecules and Nanotechnology'', Springer, Berlin, Vol. 12 of Springer Series in Biophysics, pp. 83–105, chapter 4.

Petrášek, Z., Hoege, C., Hyman, A. A., and Schwille, P. (2008a). Two-photon fluorescence imaging and correlation analysis applied to protein dynamics in *C. elegans* embryo. *Proc. SPIE* **6860,** 68601L.

Petrášek, Z., Hoege, C., Mashaghi, A., Ohrt, T., Hyman, A. A., and Schwille, P. (2008b). Characterization of protein dynamics in asymmetric cell division by scanning fluorescence correlation spectroscopy. *Biophys. J.* **95,** 5476–5486.

Petrov, E. P., and Schwille, P. (2008). State of the art and novel trends in fluorescence correlation spectroscopy. *In* ''Standardization and Quality Assurance in Fluorescence Measurements II: Bioanalytical and Biomedical Applications'', Springer, Berlin, Heidelberg, New York, Vol. 6 of Springer Series on Fluorescence, pp. 145–197.

Rička, J., and Binkert, T. (1989). Direct measurement of a distinct correlation-function by fluorescence cross-correlation. *Phys. Rev. A: At. Mol. Opt. Phys.* **39,** 2646–2652.

Ries, J., and Schwille, P. (2006). Studying slow membrane dynamics with continuous wave scanning fluorescence correlation spectroscopy. *Biophys. J.* **91,** 1915–1924.

Ries, J., Chiantia, S., and Schwille, P. (2009a). Accurate determination of membrane dynamics with line-scan FCS. *Biophys. J.* **96,** 1999–2008.

Ries, J., Yu, S. R., Burkhardt, M., Brand, M., and Schwille, P. (2009b). Modular scanning FCS quantifies receptor-ligand interactions in living multicellular organisms. *Nat. Methods* **6,** 643–645.

Rigler, R., and Elson, E. (2001). *Fluorescence Correlation Spectroscopy: Theory and Applications* Springer.

Ruan, Q., Cheng, M., Levi, M., Gratton, E., and Mantulin, W. (2004). Spatial-temporal studies of membrane dynamics: scanning fluorescence correlation spectroscopy (SFCS). *Biophys. J.* **87,** 1260–1267.

Satsoura, D., Leber, B., Andrews, D. W., and Fradin, C. (2007). Circumvention of fluorophore photobleaching in fluorescence fluctuation experiments: a beam scanning approach. *ChemPhysChem* **8,** 834–848.

Schätzel, K. (1990). Noise on photon correlation data. I. Autocorrelation functions. *Quantum Opt.* **2,** 287–305.

Schwille, P., Meyer-Almes, F., and Rigler, R. (1997). Dual-color fluorescence cross-correlation spectroscopy for multicomponent diffusional analysis in solution. *Biophys. J.* **72,** 1878–1886.

Skinner, J. P., Chen, Y., and Muller, J. D. (2005). Position-sensitive scanning fluorescence correlation spectroscopy. *Biophys. J.* **89,** 1288–1301.

Tcherniak, A., Reznik, C., Link, S., and Landes, C. F. (2009). Fluorescence correlation spectroscopy: criteria for analysis in complex systems. *Anal. Chem.* **81,** 746–754.

Thews, E., Gerken, M., Eckert, R., Zapfel, J., Tietz, C., and Wrachtrup, J. (2005). Cross talk free fluorescence cross correlation spectroscopy in live cells. *Biophys. J.* **89,** 2069–2076.

Wiseman, P. W., Squier, J. A., Ellisman, M. H., and Wilson, K. R. (2000). Two-photon image correlation spectroscopy and image cross-correlation spectroscopy. *J. Microsc.* **200,** 14–25.